

SUBSTRATE THERMAL CONDUCTIVITY CONTROLS ABILITY TO MANUFACTURE MICROSTRUCTURES VIA LASER-INDUCED DIRECT WRITE

John A. Tomko,¹ David H. Olson,² Jeffrey L. Braun,² Andrew P. Kelliher,¹ Bryan Kaehr,³ and Patrick E. Hopkins^{1,2,4,*}

¹*Department of Materials Science and Engineering, University of Virginia, Charlottesville, VA 22904, USA*

²*Department of Mechanical and Aerospace Engineering,
University of Virginia, Charlottesville, VA 22904, USA*

³*Advanced Materials Laboratory, Sandia National Laboratories, Albuquerque, New Mexico 87185, USA*

⁴*Department of Physics, University of Virginia, Charlottesville, VA 22904, USA*

(Dated: March 29, 2019)

In controlling the thermal properties of the surrounding environment, we provide insight to underlying mechanisms driving the widely-used laser direct write method for additive manufacturing. We find that the onset of silver nitrate reduction for the formation of direct write structures directly corresponds to the calculated steady-state temperature rises associated with high-repetition, ultrafast laser pulses. Furthermore, varying the geometry of the heat affected zone, which is controllable based on in-plane thermal diffusion, driven by the substrate thermal conductivity, and laser power, allows for control of the written geometries without any prior substrate preparation. These findings allow for the advance of rapid manufacturing of micro- and nanoscale structures with minimal material constraints through consideration of the laser-controllable thermal transport in ionic liquid/substrate media.

Major technological advancements in the last few decades have relied on the ability to continuously decrease the size of devices. In doing so, a dependence on manufacturing processes to enhance their spatial resolutions has grown significantly [1–4]. Optical-based techniques have been at the forefront of these processes due to the decreased length-scales associated with the ability to selectively expose materials to photon irradiation. Photolithography, for example, has been the foundation of micro- and nanoscale integrated circuits [1, 3] due to its increased spatial resolution and material compatibilities compared to typical additive manufacturing techniques (e.g., 3D printing of thermoplastics or even biomaterials [4–6]). Yet, photolithographic processes are highly limited in material capabilities/specificities as well as processing times. For example, clean-room photolithography is limited to electronic materials on a small range of substrates. Techniques that aim to address such limitations include laser-induced forward transfer (LIFT) [4, 7], laser-sintering [8, 9], and multiphoton polymerization methods [6, 10, 11].

LIFT overcomes many material limitations and is primarily used for deposition of metals and oxides [12]. Other advancements, such as the introduction of matrix-assisted laser evaporation in the direct write process (MAPLE-DW) [7], have expanded these limitations, providing the ability to create structures with far more complex materials, such as biological specimens [13]. Nonetheless, this method is not rapid enough for prototyping or mass-scale manufacturing. Furthermore, the formed structures are much larger than those created by other methods and are formed solely on planar supports. These two drawbacks arise from the requirement of a ribbon placed above the desired substrate; the formation of the ribbon is a non-trivial task, since the desired material must be pre-formed as a thin film with consistent morphology. As the ribbon must be parallel at all desired writing points on the substrate, two planar geometries are a necessity. Thus, this method does not allow for complex 3-dimensional

structures (the ribbon is consistently removed in blocks of the same size/morphology). On the other hand, laser-sintering is far less limited in geometries available, as a laser interacts with a pre-deposited powder or ink on the substrate of choice; this interaction anneals the colloidal particles or powder to form prescribed micro- and nano-structures [8, 9]. This process, however, is known to form structures with a large density of defects and poorly defined edges, as the annealing process reaches critical temperatures in the ink environment, leading to cavitation and uncontrolled growth processes [14]. Multi-photon polymerization overcomes many of the aforementioned geometry and resolution constraints, as multiphoton processes inherently occur in small volumes [15–17], but is highly limited to select materials.

Within each laser-based method, thermal effects are consistently investigated throughout the literature [4, 18, 19]. Unfortunately, many investigations fail to provide concrete evidence of a diffusive thermal processes initiating and/or driving the laser writing process. For example, previous investigations involving laser direct write from silver nitrate solutions (AgNO_3) reference photoreduction [20], multiphoton absorption [16], and even non-equilibrium growth [21] as potential factors that ultimately lead to the formation of silver structures.

As a more universally-applicable phenomenon, we investigate the role of the absorbed energy from the laser source, substrate thermal conductivity, and resulting thermal transport, on silver metal line fabrication during laser direct write on a variety of substrates submerged in an ionic liquid precursor. In our previous work, we have surmised that the local energy density and resulting steady state temperature rise from an absorbed laser source drives the thermal direct write process, and hence increases the generality and expands the material applicability of laser direct writing [22]. With the goal of producing material structures across the periodic table, wet-chemistry techniques have unveiled the proper precursor solutions for most

materials [23–27].

We hypothesize that direct control over the decomposition of the ionic liquid can be achieved through the control of heat dissipation through the substrate to limit the steady-state temperature rise resulting from laser substrate interaction. This decomposition ultimately leads to nucleation of ions, resulting in deposition of Ag structures. This thermal activation allows for universal material deposition, in terms of both the formed structure and underlying substrate, as the sole requisite for decomposition is a sufficient rise in temperature. In principle, this process theoretically allows for sub-diffraction sized structures, similar to multi-photon polymerization [10, 11], which is considered to be at the forefront of spatial resolution, as the decomposition threshold can be reached solely at the peak of the Gaussian spatial temperature distribution. Thus, the ability to control thermal directly written nanostructures via absorbed energy density that is driven by the laser source and substrate/liquid media thermal properties provides the potential to expand the current limits of fabrication of nanomaterials and hierarchical devices.

Our laser direct write method used for this work relies on a continuous-wave (CW) 532 nm laser that is focused to a $15 \mu\text{m}$ $1/e^2$ radius to form metallic Ag structures from a 0.1 M AgNO_3 ionic precursor; details on the ionic precursor preparation, as well as a diagram and additional details on the experimental setup are included in the supporting material. The peak-power density of this beam is orders of magnitude too low for multi-photon processes, such as two-photon polymerization or multi-photon absorption to occur, eliminating their potential role in the formation of Ag structures. Furthermore, thermal dissipation and accumulation of the absorbed energy density steady-state temperature rises at the solid-liquid interface are more easily quantified with knowledge of CW laser source power densities; for pulsed light sources, the large instantaneous temperature rise associated with individual pulses complicates the thermal aspect of our analysis. Thus, in this work, we use our CW 532 nm laser to demonstrate the role of steady-state temperature rises - governed by the laser power and substrate thermal conductivity - on the ability to thermally direct write metal lines on the substrate surface. As AgNO_3 has been widely studied in additive manufacturing applications [20, 28–30], it leaves a solid framework to allow for understanding of the *thermal* component of the laser direct write process, as opposed to optical interactions that impact the chemistry. Although photo-reduction of AgNO_3 into elemental Ag is known to occur, this optically-induced reduction process can be avoided, and its role in thermal direct write elucidated, by repeating the process with varying wavelengths of laser light. Thus, we repeat the direct write process using an ultrafast regenerative amplifier that emanates <500 fs pulses at 1 MHz frequency. With the addition of an optical parametric amplifier (OPA), we convert the fundamental frequency (1040 nm) into 680 nm light; this choice is well outside the spectrum of photo-reduction of AgNO_3 [31]. To elucidate control over the thermal direct write method, we attempt to write Ag on a range of substrates with varying thermal prop-

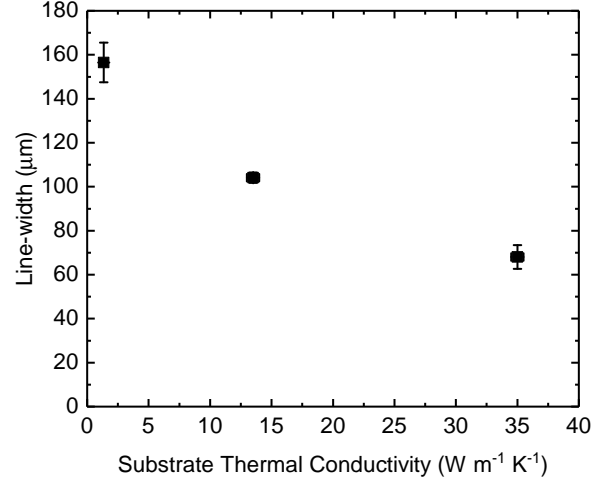


Figure 1. Measured line-width for Ag microstructures at an absorbed power density of $\sim 350 \text{ MW m}^{-2}$ for substrates of varying substrate thermal conductivity; these were synthesized with a CW 532 nm beam.

erties and find the process can be optimized based on steady-state temperature rises either from the power from the CW beam or the average accumulation the power from the laser pulses in the case of our pulsed source.

The average power from the laser absorbed on the surface of a material results in a steady-state temperature rise. We can approximate this temperature rise, ΔT , from the multilayer solution to the radially symmetric heat equation with a periodic Gaussian heat source absorbed at surface or interface, given by [32],

$$\Delta T = 2\pi P_0 \int_0^\infty G(k) \exp\left(\frac{-\pi^2 k^2 r_0^2}{2}\right) k dk \quad (1)$$

where P_0 is the absorbed laser power, r_0 is the radius of the incident beam, and $G(k)$ is the Hankel transform of the radially symmetric heat equation in a multilayer system with semi-infinite substrates. In relation to this work, this function takes into account both the thermal conductivity and the volumetric heat capacity of the substrate and overlying ionic liquid precursor, and is explained in detail in prior works [32, 33]. In the pulsed case, individual pulses are capable of much larger, impulse temperature rises on the surface in a time frame on the order of the pulse width and subsequent carrier nonequilibrium relaxation times in the material; the temperature rises associated with individual pulses are likely not a determining factor for thermal-direct write processes as the nucleation and growth mechanisms for ionic reduction occur on much larger time scales than the pulse duration used in this experiment (<500 fs), rather, the steady-state rise due to thermal accumulation from the high-repetition rate is expected to be primary mechanism for such processes [31]. Previous experimental observations for rapid particle formation via precipita-

tion have been measured via small-angle x-ray scattering, and formation is found to occur on the order of 10^2 's of μs , with further growth limited by mass transfer [34]. Furthermore, previous experiments in *laser driven* reduction have found growth to be affected by thermal accumulation at times greater than $1 \mu\text{s}$ (note: this value was determined from AgNO_3 in a gelatin matrix, where it is also predicted that negligible thermal effects occur at repetition rates of 1 MHz) [35]. Similar high-energy thermal methods for particle synthesis in liquids, such as short-pulse laser ablation, have determined the growth of nanoparticles to occur on similar time scales [36, 37]. Thus, one would predict only the cumulative effect due to multiple pulses to play a role in thermal decomposition of the ionic precursor. We find a direct correlation between the temperature rise from energy accumulation of the absorbed laser beam (Eq. 1) and the formation of structures via reduction of AgNO_3 . Thus, the hypothesis that steady-state temperature rises play the dominant role in thermal direct write, which we show is directly related to the thermal conductivity of the substrate, is further reinforced in comparing fabrication conditions between the pulsed and CW laser sources.

We write metallic lines from laser irradiation of AgNO_3 solutions on three different substrates (amorphous SiO_2 ‘glass,’ crystalline SiO_2 ‘quartz,’ and crystalline Al_2O_3 ‘sapphire’) with similar absorption coefficients at 532 and 680 nm and constant spot-size of $\sim 15 \mu\text{m}$. This greatly simplifies our thermal analysis as the steady-state temperature rise at the solid-liquid interface is dictated solely by the thermal conductivities of the fluid and substrate, as determined via Eq. 1. The resulting line-width is plotted as a function of substrate thermal conductivity in Fig. 1 for a fixed laser power density. As shown, with increasing thermal conductivity, there is a nearly linear decrease in measured line-width due to the reduced temperature rise on the substrate surface.

This posit is further supported through the measured power density thresholds to induce the direct write process with each substrate; one should expect equivalent temperature rises necessary to decompose the AgNO_3 to form metallic Ag regardless of substrate. The measured threshold necessary to form metallic Ag structures is shown in Fig. 2. In calculating these power densities, we assume $\sim 5\%$ absorption near the substrate-precursor interface; as the laser may have increased absorption due to initial structure formation (i.e., the deposited Ag line will have enhanced absorption compared to the nearly-transparent substrate), this value may be variable during the deposition process, but we expect any variability to be consistent across all substrates. This assumption is based on the extinction spectra associated with Ag nanoparticles formed from photoreduction; although considerably far from the absorption peak associated with their surface plasmon resonance, the extinction does not go to zero at 532 nm [38–40]. Additionally, silver-ion based solutions are known to have non-zero absorption at visible wavelengths [41, 42]. At a lower absorbed power density, the temperature rise is sufficiently high to laser direct-write structures on substrates with lower thermal conductivities compared to that of the sub-

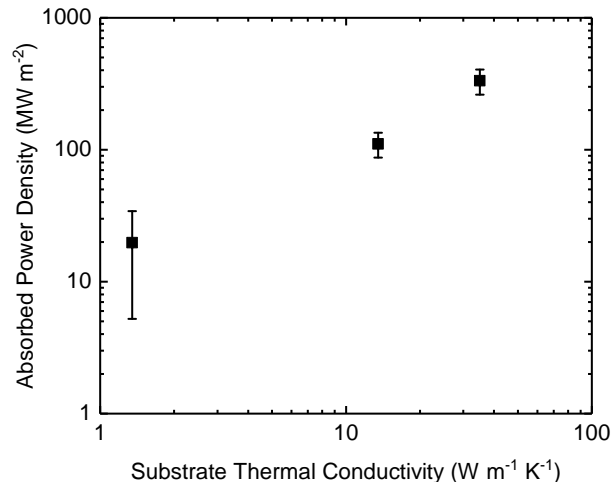


Figure 2. Measured absorbed power density necessary to form Ag microstructures on substrates (i.e., power threshold necessary to induce direct write) as a function of thermal conductivity of the substrate using a continuous wave, 532 nm beam.

strate of higher thermal conductivity. We calculate the average steady-state thermal accumulation temperature rise using the thermal conductivities of the glass, quartz and sapphire substrates measured via time domain thermoreflectance (TDTR) ($1.3 \text{ W m}^{-1} \text{ K}^{-1}$, $13.5 \text{ W m}^{-1} \text{ K}^{-1}$, and $35 \text{ W m}^{-1} \text{ K}^{-1}$, respectively) [33, 43, 44]. Furthermore, we estimate the thermal conductivity of the ionic liquid precursor to be $0.24 \text{ W m}^{-1} \text{ K}^{-1}$ based on the respective concentrations of water and ethanol (17 and 83 volume percent, respectively). In doing so, we find the maximum temperature rise at the respective power density thresholds to be within 10% of each other on all three substrates; this temperature rise being $\sim 197 \text{ K}$. Note, we reference the maximum temperature rise because it is indicative of the power density at the center of the Gaussian spatial profile associated with our laser beam. This is in reasonable agreement with previous works, where the value for thermal reduction of AgNO_3 has been measured to be as low as 150°C (equivalent to a $\sim 130 \text{ K}$ temperature rise), allowing for at least partial thermal reduction of AgNO_3 [45].

To gain further insight to the role of the steady-state temperature rises during the laser induced thermal direct-write processing, we consider the line-widths associated with varying power densities; the measured values obtained from SEM micrographs, such as shown in Fig. 3a, are depicted in Fig. 3b for fused silica and quartz substrates (with thermal conductivities of $1.3 \text{ W m}^{-1} \text{ K}^{-1}$ and $13 \text{ W m}^{-1} \text{ K}^{-1}$, respectively). As shown, there is a decrease in the width of the line with decreasing power density. This phenomenon has been demonstrated in a few previous works [28, 46]. As noted by Lu *et al.* [46], in the direct writing of Ag by thermal decomposition of CH_3COOAg , the line-width follows the temperature profile induced by the Gaussian beam. In other words, with in-

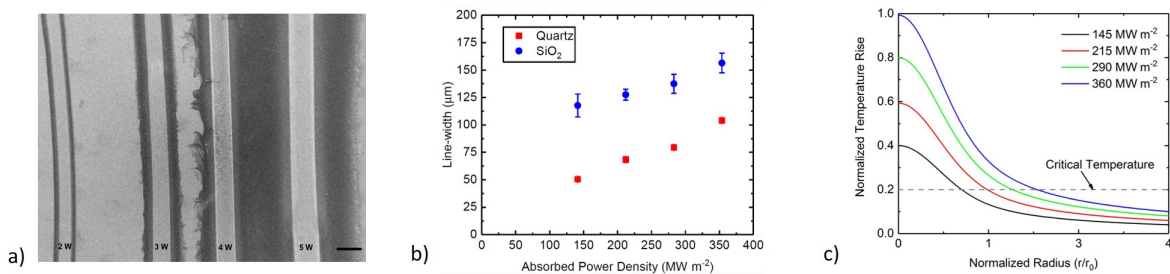


Figure 3. a) SEM micrograph of Ag structures on a quartz substrate. The scale bar is $100\ \mu\text{m}$ and the values on each Ag line are the incident laser powers. Note, the laser spot size is fixed. Additionally, the laser-produced structure contains the power label; the external formation of silver is due to photoreduction from the scattered and environmental light. b) Measured absorbed power density necessary to form Ag microstructures on substrates (i.e., power threshold necessary to induce direct write) with varying thermal conductivities. c) Normalized temperature rises at varying power densities (note, for a fixed incident radius) as a function of radius from the center of the Gaussian distribution calculated via Eq. 1.

creased laser power, the temperature threshold necessary for thermal decomposition of the precursor liquid is exceeded at distances farther from the center of the beam profile. This concept is further reinforced through consideration of Eq. 1; we plot the calculated temperature profile as a function of radius from the center of the Gaussian distribution in Fig. 3c. As can be seen, with increasing power density, the critical temperature rise necessary to induce thermal decomposition of the precursor is obtained at increasing distances from the center of the incident beam. As an additional experiment to vary the steady-state temperature rise and investigate its role during laser thermal direct write manufacturing, we alter the dwell time (i.e., scan velocity) of the incident beam. As discussed in detail in the supporting material, and graphically depicted in Fig. S2, we find a decrease in line-width, or lower induced temperature rise across the Gaussian distribution, with decreased dwell times/increased scan velocities, as one would predict via Eq. 1.

Although the role of the substrate thermal conductivity and resulting temperature rise as a method for laser direct writing of nanostructures is clearly demonstrated above, in addition to the fact we utilize a low peak-power, CW beam to negate the potential for multi-photon processes, we cannot rule out an initiation process being driven by photo-decomposition of the silver nitrate solution. To gain insight into the role of photodecomposition and further thermal processing, we thermally direct write with a pulsed laser at 680 nm. Additionally, should photoreduction be a prominent mechanism, the reduced photon energy should present different results as compared to the case of the visible light at 532 nm.

In the case of $<500\ \text{fs}$ pulses heating the sample at a frequency of 1 MHz, we continue to find a similar trend in power thresholds and associated line widths for silver structures on the three substrates with varying thermal conductivities. For example, due to the non-linear processes necessary to reach near-infrared wavelengths through the OPA, the available average power output is limited in this experimental scheme, and we are unable to thermally write structures on sapphire due to its high thermal conductivity and thus low steady-state

temperature rise even at the maximum attainable power density. This finding further reinforces the notion of thermal decomposition rather than photodecomposition of the AgNO_3 to metallic Ag. Conversely, glass reaches high enough temperatures for rapid decomposition of AgNO_3 and subsequent nucleation of metallic silver. Crystalline quartz, with an order of magnitude larger thermal conductivity as compared to the SiO_2 glass (and thus lower steady-state temperature rise at the solid-liquid interface), only undergoes partial decomposition of silver nitrate, leading to minimal nucleation [45]. Although photo-decomposition may be operating in tandem with thermal reduction of the precursor, the agreement between varying wavelengths in both a pulsed and continuous-wave laser implies the role of thermal accumulation can not be ignored.

In conclusion, we have demonstrated that thermal accumulation at the solid-liquid interface of the desired substrate and ionic liquid precursor is a primary mechanism for the direct write processing of micro- and nano-structures. Compared to previous works that rely on multi-photon processes, photoreists and multi-step processing, thermal direct write is a useful one step method for rapid synthesis of well-defined structures as direct write can be achieved simply through the addition of a liquid precursor atop the desired substrate. Additionally, AgNO_3 has previously only been directly written to substrates with an adhesion layer such as a silane-coating added prior to the deposition [16, 35]; with thermal direct write, we find that no substrate preparation is necessary. This evidence also provides a future pathway for enhancement and optimization of additive manufacturing techniques relying on laser-material interactions, particularly due to the inherent thermal effects associated with any laser-matter interaction. Through management of thermal dissipation within the laser-induced heat-affected zone, control of morphology, deposition rate, and volume of the formed structure can be controlled with increased precision.

See supplementary material for details on experimental methods including the ionic precursor and substrate preparation procedures, additional details, including a diagram, on the experimental setup, as well as additional information on

the characterization performed.

We appreciate support from the Office of Naval Research, Grant. No. N00014-15-12769

* phopkins@virginia.edu

- [1] R. P. Seisyan, *Technical Physics* **56**, 1061 (2011).
- [2] A. Piqué, D. W. Weir, P. K. Wu, B. Pratap, C. B. Arnold, B. R. Ringeisen, R. A. McGill, R. C. Y. Auyeung, R. A. Kant, and D. B. Chrisey, *Photon Processing in Microelectronics and Photonics* **4637**, 361 (2002).
- [3] R. F. Pease and S. Y. Chou, *Proceedings of the IEEE* **96**, 248 (2008).
- [4] C. B. Arnold, P. Serra, and A. Piqué, *MRS Bulletin* **32**, 23 (2007).
- [5] A. Selimis, V. Mironov, and M. Farsari, *Microelectronic Engineering* **132**, 83 (2014).
- [6] H. N. Chia and B. M. Wu, *Journal of Biological Engineering* **9**, 4 (2015).
- [7] A. Piqué, D. B. Chrisey, R. C. Y. Auyeung, J. Fitz-Gerald, H. D. Wu, R. A. McGill, S. Lakeou, P. K. Wu, V. Nguyen, and M. Duignan, *Applied Physics A: Materials Science and Processing* **69**, 279 (1999).
- [8] S. H. Ko, H. Pan, C. P. Grigoropoulos, C. K. Luscombe, J. M. J. Fréchet, and D. Poulikakos, *Nanotechnology* **18**, 345202 (2007).
- [9] M. Agarwala, D. Bourell, J. Beaman, H. Marcus, and J. Barlow, *Rapid Prototyping Journal* **1**, 26 (1995), arXiv:arXiv:1011.1669v3.
- [10] L. L. Erskine, A. a. Heikal, S. M. Kuebler, M. Rumi, X.-I. Wu, S. R. Marder, and J. W. Perry, *Solid State Physics* **398**, 51 (1999).
- [11] J. Serbin, A. Egbert, A. Ostendorf, B. N. Chichkov, R. Houbertz, G. Domann, J. Schulz, C. Cronauer, L. Fröhlich, and M. Popall, *Optics Letters* **28**, 301 (2003).
- [12] P. Delaporte and A.-P. Alloncle, *Optics & Laser Technology* **78**, 33 (2016).
- [13] P. Serra, M. Colina, J. M. Fernández-Pradas, L. Sevilla, and J. L. Morenza, *Applied Physics Letters* **85**, 1639 (2004).
- [14] S. A. Khairallah, A. T. Anderson, A. Rubenchik, and W. E. King, *Acta Materialia* **108**, 36 (2016), arXiv:arXiv:1011.1669v3.
- [15] X.-L. Ren, M.-L. Zheng, F. Jin, Y.-Y. Zhao, X.-Z. Dong, J. Liu, H. Yu, X.-M. Duan, and Z.-S. Zhao, *The Journal of Physical Chemistry C* **120**, 26532 (2016).
- [16] T. Baldacchini, A.-C. Pons, J. Pons, C. N. LaFratta, J. T. Fourkas, Y. Sun, and M. J. Naughton, *Optics Express* **13**, 1275 (2005).
- [17] M. Deubel, G. von Freymann, M. Wegener, S. Pereira, K. Busch, and C. M. Soukoulis, *Nature Materials* **3**, 444 (2004).
- [18] S. S. Chou, B. S. Swartzentruber, M. T. Janish, K. C. Meyer, L. B. Biedermann, S. Okur, D. B. Burckel, C. B. Carter, and B. Kaehr, *The Journal of Physical Chemistry Letters* **7**, 3736 (2016).
- [19] S. D. Gittard and R. J. Narayan, *Expert Review of Medical Devices* **7**, 343 (2010), arXiv:NIHMS150003.
- [20] S. Maruo and T. Saeki, *Optics express* **16**, 1174 (2008).
- [21] K. Vora, S. Kang, M. Moebius, and E. Mazur, *Applied Physics Letters* **105**, 1 (2014).
- [22] L. D. Zarzar, B. S. Swartzentruber, B. F. Donovan, P. E. Hopkins, and B. Kaehr, *ACS Applied Materials and Interfaces* **8**, 21134 (2016).
- [23] S. G. Kwon and T. Hyeon, *Accounts of Chemical Research* **41**, 1696 (2008).
- [24] H. Winnischofer, T. C. R. Rocha, W. C. Nunes, L. M. Socolovsky, M. Knobel, and D. Zanchet, *ACS nano* **2**, 1313 (2008).
- [25] Z. Lu and Y. Yin, *Chemical Society Reviews* **41**, 6874 (2012).
- [26] R. Shankar, B. B. Wu, and T. P. Bigioni, *The Journal of Physical Chemistry C* **114**, 15916 (2010).
- [27] K. Riwozki and M. Haase, *The Journal of Physical Chemistry B* **102**, 10129 (1998).
- [28] M. A. Skylar-scott, S. Gunasekaran, and J. A. Lewis, *Proceedings of the National Academy of Sciences* **113**, 6137 (2016).
- [29] V. Bromberg, S. Ma, F. D. Egitto, and T. J. Singler, *Journal of Materials Chemistry C* **1**, 6842 (2013).
- [30] H.-j. Chang, M.-h. Tsai, W.-s. Hwang, J.-t. Wu, S. L.-c. Hsu, and H.-h. Chou, *The Journal of Physical Chemistry C* **116**, 4612 (2012).
- [31] H. Tanimoto, S. Ohmura, and Y. Maeda, *Journal of Physical Chemistry C* **116**, 15819 (2012).
- [32] J. L. Braun and P. E. Hopkins, *Journal of Applied Physics* **175107**, 1 (2017).
- [33] D. G. Cahill, *Review of Scientific Instruments* **75**, 5119 (2004).
- [34] W. Schmidt, P. Bussian, M. Lindén, H. Amenitsch, P. Agren, M. Tiemann, and F. Schüth, *Journal of the American Chemical Society* **132**, 6822 (2010).
- [35] K. Vora, *Three-dimensional nanofabrication of silver structures in polymer with direct laser writing*, Ph.D. thesis (2014).
- [36] P. Wagnen, S. Ibrahimkuty, A. Menzel, A. Plech, and S. Barcikowski, *Phys. Chem. Chem. Phys.* **15**, 3068 (2013).
- [37] J. Tomko, S. M. O'Malley, C. Trout, J. J. Naddeo, R. Jimenez, J. C. Gripenburg, W. Soliman, and D. M. Bubb, *Colloids and Surfaces A: Physicochemical and Engineering Aspects* **522**, 368 (2017).
- [38] M. Ratti, Y. Tan, J. J. Naddeo, J. C. Gripenburg, J. Tomko, C. Trout, S. M. O. Malley, D. M. Bubb, and E. A. Klein, *Applied Physics A*, 1 (2016).
- [39] L. Kvítek, A. Panáček, J. Soukupová, M. Kolář, R. Večeřová, R. Prucek, M. Holecová, and R. Zbořil, *Journal of Physical Chemistry C* **112**, 5825 (2008).
- [40] M. G. M. Guzmán, J. Dille, and S. Godet, *International Scholarly and Scientific Research & Innovation* **2**, 91 (2008).
- [41] W. Zhou, S. Bai, Y. Ma, D. Ma, T. Hou, X. Shi, and A. Hu, *ACS Applied Materials and Interfaces* **8**, 24887 (2016).
- [42] C. M. Völkle, D. Gebauer, and H. Cölfen, *Faraday Discuss.* **179**, 59 (2015).
- [43] A. J. Schmidt, X. Chen, and G. Chen, *Review of Scientific Instruments* **79**, 1 (2008).
- [44] P. E. Hopkins, J. C. Duda, B. Kaehr, X. W. Zhou, C. Y. Peter Yang, and R. E. Jones, *Applied Physics Letters* **103**, 1 (2013).
- [45] J. W. Kwon, S. H. Yoon, S. S. Lee, K. W. Seo, and I. W. Shim, *Bulletin of the Korean Chemical Society* **26**, 837 (2005).
- [46] Y.-F. Lu, M. Takai, S. Nagatomo, K. Kato, and S. Namba, *Applied Physics A* **54**, 51 (1992).